



# A semi-naphthorhodafluor-based red-emitting fluorescent probe for tracking of hydrogen polysulfide in living cells and zebrafish



Yingying Ma <sup>a,b</sup>, Zhencai Xu <sup>b</sup>, Qi Sun <sup>c</sup>, Linlin Wang <sup>a,b</sup>, Heng Liu <sup>a,b,\*</sup>, Fabiao Yu <sup>b,\*</sup>

<sup>a</sup> Ministry of Education Key Laboratory for the Synthesis and Application of Organic Functional Molecules, College of Chemistry and Chemical Engineering, Hubei University, Wuhan 430062, China

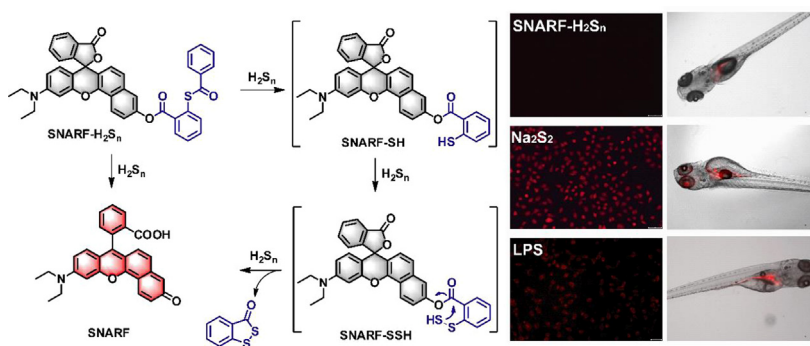
<sup>b</sup> Key Laboratory of Emergency and Trauma, Ministry of Education, Key Laboratory of Hainan Trauma and Disaster Rescue, The First Affiliated Hospital of Hainan Medical University, Institute of Functional Materials and Molecular Imaging, College of Emergency and Trauma, Hainan Medical University, Haikou 571199, China

<sup>c</sup> Key Laboratory for Green Chemical Process of Ministry of Education and School of Chemistry and Environmental Engineering, Wuhan Institute of Technology, Wuhan 430205, China

## HIGHLIGHTS

- A semi-naphthorhodafluor-based red-emitting fluorescent probe SNARF-H<sub>2</sub>S<sub>n</sub> for selective detection of H<sub>2</sub>S<sub>n</sub> was designed.
- The addition of H<sub>2</sub>S<sub>n</sub> would result in a > 1000-fold fluorescence enhancement within 10 min.
- SNARF-H<sub>2</sub>S<sub>n</sub> was successfully employed to image exogenous/endogenous H<sub>2</sub>S<sub>n</sub> in living cells and zebrafish.

## GRAPHICAL ABSTRACT



## ARTICLE INFO

### Article history:

Received 29 September 2020

Received in revised form 13 October 2020

Accepted 13 October 2020

Available online 24 October 2020

### Keywords:

Fluorescent probes  
 Hydrogen polysulfide  
 Red-emitting  
 Cell imaging  
 In vivo imaging

## ABSTRACT

Hydrogen polysulfides (H<sub>2</sub>S<sub>n</sub>, n ≥ 2) is recently regarded as a potential signaling molecule which shows a higher efficiency than hydrogen sulfides (H<sub>2</sub>S) in regulating enzymes and ion channels. However, the development of specific fluorescent probes for H<sub>2</sub>S<sub>n</sub> with long-wavelength emission (>600 nm) are still rare. In this work, a semi-naphthorhodafluor-based red-emitting fluorescent probe SNARF-H<sub>2</sub>S<sub>n</sub> containing a phenyl 2-(benzoylthio) benzoate responsive unit was constructed. SNARF-H<sub>2</sub>S<sub>n</sub> was capable of selectively detecting H<sub>2</sub>S<sub>n</sub> over other reactive sulfur species. Treatment with H<sub>2</sub>S<sub>n</sub> would result in a > 1000-fold fluorescence enhancement within 10 min. SNARF-H<sub>2</sub>S<sub>n</sub> showed a low limit of detection down to 6.7 nM, and further enabled to visualize exogenous/endogenous H<sub>2</sub>S<sub>n</sub> in living A549 cells and zebrafish.

© 2020 Elsevier B.V. All rights reserved.

## 1. Introduction

Reactive sulfur species (RSS), consisting of thiols, hydrogen sulfides (H<sub>2</sub>S), S-modified protein cysteine adducts, hydrogen polysulfides (H<sub>2</sub>S<sub>n</sub>, n ≥ 2) and so on, are playing an indispensable role in biomedical research [1–4]. Among them, there has been a great deal of interest in the study of H<sub>2</sub>S in the past decades. Extensive studies have been revealed H<sub>2</sub>S can contribute to a large body of

\* Corresponding authors at: Key Laboratory of Emergency and Trauma, Ministry of Education, Key Laboratory of Hainan Trauma and Disaster Rescue, The First Affiliated Hospital of Hainan Medical University, Institute of Functional Materials and Molecular Imaging, College of Emergency and Trauma, Hainan Medical University, Haikou 571199, China.

E-mail addresses: [liuheng@hainmc.edu.cn](mailto:liuheng@hainmc.edu.cn) (H. Liu), [yufabiao@hainmc.edu.cn](mailto:yufabiao@hainmc.edu.cn) (F. Yu).

physiological and pathological processes, such as protection against oxidative stresses [5,6], regulation of blood vessel tone [7]. The  $H_2S$  level variations will result in a series of diseases ranging from hypertension to diabetes, Down's syndrome and Alzheimer's diseases [8–10]. Recently,  $H_2S_n$  have successfully aroused widespread attention chiefly because evidences show that  $H_2S_n$  plays a more important role than  $H_2S$  in mediating certain biological mechanisms [11,12]. Much of what we know about  $H_2S$  as a signaling molecule may actually be attributed to  $H_2S_n$  [13].  $H_2S_n$  can be endogenously produced from the reaction of  $H_2S$  and reactive oxygen species like hypochlorite and can form redox couples with  $H_2S$  coexisting in biological systems [14].  $H_2S_n$  exerts an enormous function on redox biology and is associated with a large body of physiological processes. Thus, the development of accurate and highly selective methods to monitor  $H_2S_n$  levels in living organisms is necessary for an in-depth understanding of its production, degradation pathway and regulatory mechanisms.

Mass spectrometry and UV-vis spectroscopy are commonly employed for the determination of  $H_2S_n$ , but these tradition methods cannot achieve in-situ measurement of  $H_2S_n$  in cells or in vivo [15,16]. In this case, fluorescent probes are selected as potentially powerful tools for tracking  $H_2S_n$  in living organisms due to its high spatial and temporal resolution [17–23]. Inspired by pioneering work of Xian's group, several fluorescent probes for  $H_2S_n$  have been reported on basis of different response units, which mainly include 2-fluoro-5-nitrobenzoic ester [24–31], aziridine [32], nitro [33–36], phenyl 2-(benzoylthio) benzoate [37–40], and cinnamate ester [41]. However, 2-fluoro-5-nitrobenzoic ester, aziridine and cinnamate ester may be attacked by nucleophiles to cause probe consumption, and nitro may be reduced by other reducing species such as  $H_2S$ , carbon monoxide [42,43]. Moreover, there are still some other issues to sort out, such as poor selectivity, low sensitivity or limitations in vivo applications. Hence, the development of ideal fluorescent probes for  $H_2S_n$  detection are still desirable.

Encouraged by the above considerations, we herein designed and synthesized a simple semi-naphthorhodafluor-based red-emitting fluorescent probe, namely SNARF- $H_2S_n$ , for specific tracking of  $H_2S_n$ . The probe SNARF- $H_2S_n$  bearing phenyl 2-(benzoylthio) benzoate as a responsive unit showed a remarkable fluorescence off-on response to  $H_2S_n$ . We reasoned that SNARF- $H_2S_n$  enabled the release SNARF fluorophore due to the unique dual-reactivity of  $H_2S_n$ , thus triggering the dramatic fluorescence changes. Furthermore, to illustrate the potential application of SNARF- $H_2S_n$ , we have successfully applied this probe for imaging exogenous/endogenous  $H_2S_n$  in living A549 cells and zebrafish.

## 2. Experimental section

### 2.1. General method

Unless otherwise noted, the reagents and solvent in this work were commercially available and were used without further purification. Ultrapure water (18.2 M $\Omega$ -cm) was used for all spectral analysis.  $^1H$  NMR and  $^{13}C$  NMR spectra were measured on a Varian 600 MHz spectrometer as solutions in  $CDCl_3$ . High-resolution mass spectra (HRMS) were recorded on a Bruker Solarix in positive mode. UV-vis absorption and fluorescence spectra were performed on commercial spectrophotometers (Shimadzu UV-2700 and Agilent Cary Eclipse spectrophotometer). Cell images were obtained on an inverted fluorescence microscope (Olympus IX71, Japan). Zebrafish images were acquired on a stereomicroscope (Olympus SZX16, Japan). A stock solution of SNARF- $H_2S_n$  (1 mM) in dimethyl sulfoxide was prepared. The stock solution (10 mM) of various potential biological analytes, such as reactive sulfur species (Cys, GSH, Hcy,  $CH_3SSSCH_3$ , GSSG,  $Na_2S$ ,  $Na_2S_2O_3$ ,  $Na_2SO_3$ ,  $Na_2SO_4$ ,

$Na_2S_2$ ), common amino acids (Ile, Ala, Arg, Gly, Ser, Pro) and L-ascorbic acid were prepared in ultrapure water. The stock solution (10 mM) of  $CH_3SSSCH_3$  was prepared in acetonitrile. The stock solution (5 mM) of  $S_8$  was prepared in ethanol. The solution of reactive oxygen species ( $H_2O_2$ ,  $O_2^-$ ,  $\cdot OH$ ,  $^1O_2$ ,  $ClO^-$ ) were prepared according to the previous literatures [40]. All the spectra were measured in PBS buffer (50 mM, pH 7.4, containing 100  $\mu M$  CTAB). The fluorescence was obtained upon the excitation of 580 nm. The excitation and emission slits were set at 5 nm/5 nm. PMT detector voltage = 600 V.

### 2.2. Fluorescence imaging in living cells

A549 human lung carcinoma cells were cultured in Dulbecco's modified eagle's medium (DMEM) medium supplemented with 10% (v/v) fetal bovine serum and 1% (v/v) penicillin-streptomycin with an atmosphere containing 5% carbon dioxide at 37  $^\circ C$ . A549 cells were incubated with DMEM culture medium containing 10  $\mu M$  SNARF- $H_2S_n$  and 50  $\mu M$  CTAB for 30 min. A549 cells stained with 50  $\mu M$   $Na_2S_2$  and 50  $\mu M$  CTAB for 30 min were treated with 10  $\mu M$  SNARF- $H_2S_n$  for another 30 min. A549 cells stimulated with LPS for 12 h, and then incubated with 10  $\mu M$  SNARF- $H_2S_n$  for 30 min. The cells were washed with DMEM for three times, and then applied for fluorescence imaging measurements on an inverted fluorescence microscope (Olympus IX71, Japan).

### 2.3. Fluorescence imaging in larval zebrafish

The zebrafish larvae post-fertilization obtained from Eze-Rinka Company (Nanjing, China) were kept in 10 ml of embryonic medium supplemented with 1-phenyl-2-thiourea in a beaker at 30  $^\circ C$  for 96 h. The fluorescence imaging in larval zebrafish were divided into four groups. First group: the 5-day-old zebrafish alone were the control group. Second group: the zebrafish were stained with 10  $\mu M$  SNARF- $H_2S_n$  for 30 min. Third group: the zebrafish were stained with 50  $\mu M$   $Na_2S_2$  for 1 h, and further incubated with 10  $\mu M$  SNARF- $H_2S_n$  for 30 min. Fourth group: the zebrafish stimulated with LPS for 12 h, and then incubated with 10  $\mu M$  SNARF- $H_2S_n$  for 30 min. The zebrafish were washed with PBS for three times, and then applied for fluorescence imaging measurements on a stereomicroscope (Olympus SZX16, Japan).

### 2.4. Synthesis of SNARF- $H_2S_n$

SNARF- $H_2S_n$  was synthesized by the reaction of SNARF with 2-(benzoylthio)benzoic acid according to the reported literatures [44]. To a stirred solution of SNARF (43.8 mg, 0.1 mmol), 2-(benzoylthio)benzoic acid (30.9 mg, 0.12 mmol), 1-(3-dimethylaminopropyl)-3-ethylcarbodiimide hydrochloride (28.7 mg, 0.15 mmol) in methylene chloride (5 ml) was added 4-dimethylaminopyridine (2.4 mg, 0.02 mol). The mixture was stirred under Ar at room temperature for 6 h. The solution was evaporated in vacuum and the residue was purified by column chromatography on silica gel (methylene chloride/methanol = 30/1) to afford the desired product SNARF- $H_2S_n$  as a pink solid (52.3 mg, yield 77%). SNARF- $H_2S_n$   $^1H$  NMR (600 MHz,  $CDCl_3$ ):  $\delta$  8.62 (d,  $J$  = 9.1 Hz, 1H), 8.29 (d,  $J$  = 7.6 Hz, 1H), 8.04 (d,  $J$  = 7.9 Hz, 3H), 7.73 (d,  $J$  = 7.6 Hz, 1H), 7.67–7.57 (m, 6H), 7.49–7.45 (m, 3H), 7.34 (d,  $J$  = 8.7 Hz, 1H), 7.14 (d,  $J$  = 7.5 Hz, 1H), 6.76 (d,  $J$  = 8.7 Hz, 1H), 6.65 (d,  $J$  = 9.0 Hz, 1H), 6.63 (d,  $J$  = 2.0 Hz, 1H), 6.42 (dd,  $J$  = 9.0, 2.1 Hz, 1H), 3.40 (q,  $J$  = 7.1 Hz, 4H), 1.21 (t,  $J$  = 7.1 Hz, 6H);  $^{13}C$  NMR (150 MHz,  $CDCl_3$ ):  $\delta$  189.28, 169.70, 164.65, 153.65, 152.37, 149.93, 149.55, 147.42, 137.22, 136.45, 134.93, 134.85, 133.88, 133.77, 132.57, 131.57, 129.63, 129.48, 128.87, 128.83, 128.76, 127.54, 126.95, 125.06, 124.84, 124.13, 124.02, 122.56, 122.00, 121.36, 118.64, 112.74, 108.89, 104.95, 97.66, 84.26, 44.45,

12.53; HRMS  $m/z$ :  $C_{42}H_{31}NO_6S$   $[M+H]^+$  calcd for 678.1950 found 678.1947.

### 3. Results and discussion

#### 3.1. Molecular design and synthesis

SNARF, a semi-naphthorhodafluor red-emitting dye, was selected due to its desirable optical properties such as long-wavelength emission ( $>600$  nm), good photostability, moderate Stokes shift and fluorescence quantum yield. The spiroactone ring structure changes of SNARF could trigger obvious color changes, which was easily observed by naked-eyes and potentially applied for visual detection. Thus, SNARF was commonly used in the construction of functional fluorescent probes. As reported,  $H_2S_n$  possessed a unique dual reactivity including electrophilicity and nucleophilicity. Based on the dual reactivity of  $H_2S_n$ , we designed and prepared a SNARF-based off-on fluorescent probe for sensing  $H_2S_n$  by tagging a  $H_2S_n$ -specific response unit phenyl 2-(benzoylthio) benzoate to SNARF scaffold. SNARF- $H_2S_n$  was synthesized via a two-step reaction, and its structure was determined by  $^1H$  NMR,  $^{13}C$  NMR and HRMS. As depicted in Scheme 1, the reaction of SNARF- $H_2S_n$  and  $H_2S_n$  took place in three steps: (i)  $H_2S_n$  acted as a nucleophile to attack phenyl 2-(benzoylthio) benzoate to form intermediate SNARF-SH; (ii) SNARF-SH was trapped by  $H_2S_n$  as an electrophile to generate SNARF-SSH; (iii) SNARF-SSH released the fluorophore SNARF and by-products benzodithiolone through intramolecular cyclization. To confirm the sensing mechanism, the reaction of SNARF- $H_2S_n$  with  $H_2S_n$  was performed in the acetonitrile/PBS buffer ( $v/v = 1:1$ , 50 mM, pH 7.4, containing 100  $\mu M$  CTAB). As a result, SNARF and benzodithiolone were obtained with good yield.

#### 3.2. Response performances of SNARF- $H_2S_n$

With SNARF- $H_2S_n$  in hand, we first evaluated the spectral performance in 50 mM phosphate buffer solution (pH 7.4, containing 100  $\mu M$  CTAB). Surprisingly, SNARF- $H_2S_n$  was non-emissive before addition of  $H_2S_n$  upon excitation at 580 nm. The fluorescence emission centered at 640 nm exhibited a gradual increase by adding various amounts of  $H_2S_n$  (0–50  $\mu M$ ) (Fig. S4). Upon addition of  $H_2S_n$  (25  $\mu M$ ), SNARF- $H_2S_n$  fluorescence reached the maximum, showing a  $> 1000$ -fold enhancement compared to free SNARF- $H_2S_n$  (Fig. 1a). Particularly, an excellent linear relationship ( $F_{640\text{ nm}} = 13.96 \times [Na_2S_2] \mu M + 0.1559$ ,  $R^2 = 0.9983$ ) within the  $H_2S_n$  concentration range of 0–20  $\mu M$  was obtained, and the limit of

detection (LOD =  $3\sigma/k$ ) was found to be 6.7 nM (Fig. 1b, S5). Such a low detection limit was below most of the previous reported  $H_2S_n$  probes, which also demonstrated SNARF- $H_2S_n$  was potentially used for tracking low concentration levels of  $H_2S_n$  in living organisms (Table S1). The time course of the reaction of SNARF- $H_2S_n$  with  $H_2S_n$  was also investigated (Fig. 1c). Over 10 min, the emission intensity ( $\lambda_{em} = 640$  nm) of SNARF- $H_2S_n$  was close to saturation. Therefore, we chose 10 min as the response time for spectral analysis. Furthermore, we explored the effects of different pH values on the reactivity of SNARF- $H_2S_n$  toward  $H_2S_n$ . As can be seen in Fig. 1d, SNARF- $H_2S_n$  fluorescence was weak and remained constant, revealing SNARF- $H_2S_n$  was very stable over a range of pH 3.0–11.0. In the presence of  $H_2S_n$ , a drastic increase in the emission intensity ( $\lambda_{em} = 640$  nm) at pH levels of 6.0–11.0. The obtained results illustrated SNARF- $H_2S_n$  enabled to sense  $H_2S_n$  under the normal physiological range.

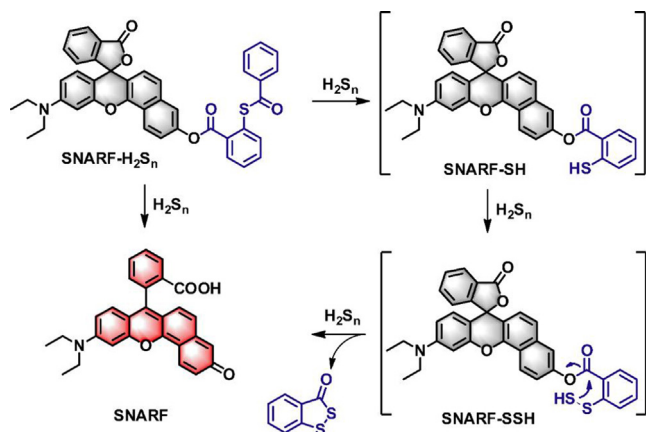
Selectivity was one of the important criteria to evaluate the sensing performance of the probe. Next, treating SNARF- $H_2S_n$  with various potential biological analytes, such as reactive sulfur species (Cys, GSH, Hcy,  $CH_3SSSCH_3$ , GSSG,  $Na_2S$ ,  $Na_2S_2O_3$ ,  $Na_2SO_3$ ,  $Na_2SO_4$ ,  $S_8$ ), common amino acids (Ile, Ala, Arg, Gly, Ser, Pro) and L-ascorbic acid, to evaluate the selectivity of SNARF- $H_2S_n$  toward  $H_2S_n$ . Based on the obtained results from Fig. 1e, other biological analytes could hardly trigger SNARF- $H_2S_n$  fluorescence change except  $Na_2S_2$ . It was reported that  $H_2S_n$  might be produced from the reaction between  $H_2S$  and reactive oxygen species (ROS) in living system. To validate the scenario, we chose various ROS including  $H_2O_2$ ,  $O_2^-$ ,  $\cdot OH$ ,  $^1O_2$  and  $ClO^-$  to carry out the following tests. As shown in Fig. 1f, insignificant changes in the emission intensity ( $\lambda_{em} = 640$  nm) of SNARF- $H_2S_n$  were seen in the presence of ROS. However, after mixing ROS and  $H_2S$ , SNARF- $H_2S_n$  showed varying degrees of fluorescence response, especially the addition of  $ClO^-$  induced a remarkable fluorescence intensity change. These results clarified the excellent selectivity of SNARF- $H_2S_n$  toward  $H_2S_n$  and possible biosynthetic pathway of  $H_2S_n$ .

#### 3.3. Cellular fluorescence imaging

The excellent spectroscopic response performance prompted us to explore whether SNARF- $H_2S_n$  was capable of monitoring exogenous/endogenous  $H_2S_n$  by fluorescence microscope. Prior to cellular imaging experiments, a standard CCK-8 assay was carried out to explore the cytotoxicity of SNARF- $H_2S_n$  on A549 cells. Results from Fig. S6 showed the cells maintained a high cell viability when the concentration of SNARF- $H_2S_n$  increased to 20  $\mu M$ . It was clearly seen from Fig. 2a that almost no fluorescence signal was observed after addition of SNARF- $H_2S_n$ , demonstrating the low level of  $H_2S_n$  in A549 cells. As a control, the cells sequentially stained with  $Na_2S_2$  and SNARF- $H_2S_n$  presented a very strong fluorescence signal. As reported, cystathionine g-lyase (CSE) mRNA could be overexpressed by the stimulation of lipopolysaccharides (LPS), expediting the production of endogenous  $H_2S_n$ . Therefore, the effect of incubation of LPS stimulation on the production of  $H_2S_n$  in A549 cells was evaluated. When the cells stimulated with LPS for 12 h, and then incubated with SNARF- $H_2S_n$ , the increase in fluorescence was seen in Fig. 2b, which indicated LPS could induce the upregulation of  $H_2S_n$ . These results demonstrated SNARF- $H_2S_n$  featured excellent biocompatibility and enabled effectively to track exogenous/endogenous  $H_2S_n$  in cells.

#### 3.4. In vivo fluorescence imaging

Furthermore, in order to inquiry the potential of SNARF- $H_2S_n$  for imaging  $H_2S_n$  in vivo, we selected larval zebrafish as a model organism because of its similar genetic structure with human. As displayed in Fig. 3a, the fluorescence of SNARF- $H_2S_n$ -stained zebra-



Scheme 1. Reaction mechanism of SNARF- $H_2S_n$  toward  $H_2S_n$ .

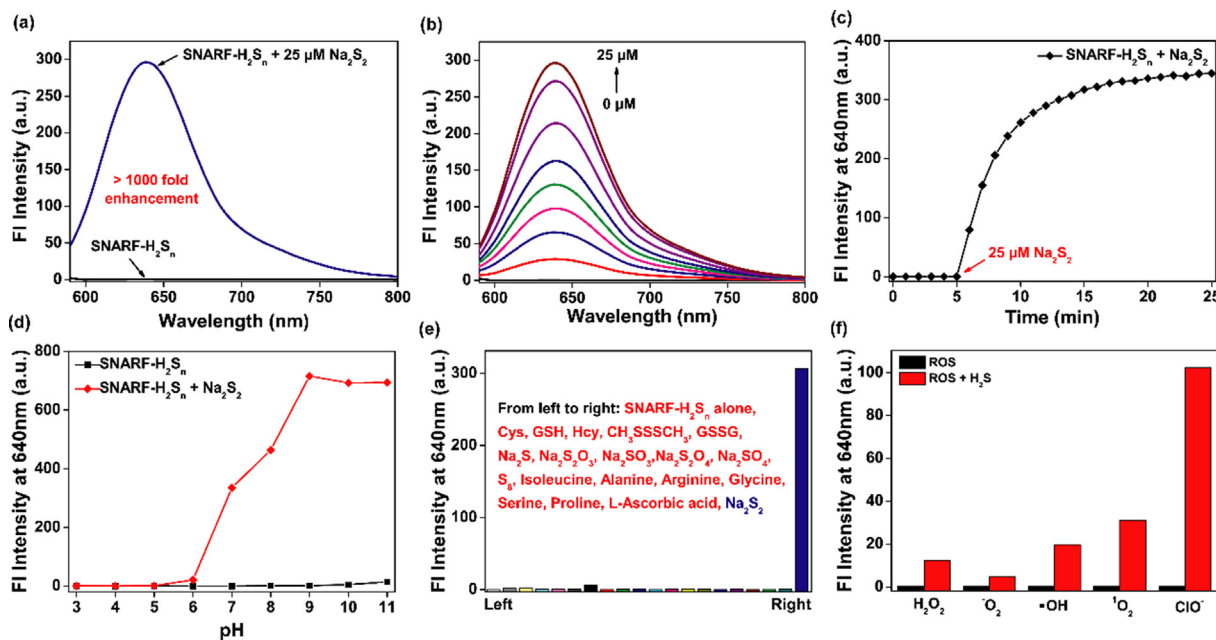


**Fig. 1.** (a) Fluorescence spectra of SNARF-H<sub>2</sub>S<sub>n</sub> (10 μM) in the presence and absence of Na<sub>2</sub>S<sub>2</sub> (25 μM). (b) Fluorescence responses of SNARF-H<sub>2</sub>S<sub>n</sub> (10 μM) upon addition of Na<sub>2</sub>S<sub>2</sub> (0–25 μM) for 10 min. (c) Time courses of fluorescence intensities at 640 nm before and after addition of Na<sub>2</sub>S<sub>2</sub> (25 μM). (d) Influence of pH on the response of SNARF-H<sub>2</sub>S<sub>n</sub> (10 μM) in the presence and absence of Na<sub>2</sub>S<sub>2</sub> (25 μM). (e) Fluorescence responses of SNARF-H<sub>2</sub>S<sub>n</sub> (10 μM) at 640 nm toward various potential biological analytes. From left to right: blank, Cys (200 μM), GSH (1 mM), Hcy (200 μM), CH<sub>3</sub>SSSCH<sub>3</sub> (100 μM), GSSG (100 μM), Na<sub>2</sub>S (100 μM), Na<sub>2</sub>S<sub>2</sub>O<sub>3</sub> (100 μM), Na<sub>2</sub>SO<sub>3</sub> (100 μM), Na<sub>2</sub>SO<sub>4</sub> (100 μM), S<sub>8</sub> (50 μM), Ile (100 μM), Ala (100 μM), Arg (100 μM), Gly (100 μM), Ser (100 μM), Pro (100 μM), L-ascorbic acid (100 μM), Na<sub>2</sub>S<sub>2</sub> (25 μM). (f) Fluorescence responses of SNARF-H<sub>2</sub>S<sub>n</sub> (10 μM) at 640 nm in the presence of ROS (with or without 100 μM Na<sub>2</sub>S). From left to right: H<sub>2</sub>O<sub>2</sub> (200 μM), (2) O<sub>2</sub> (100 μM), ·OH (100 μM), <sup>1</sup>O<sub>2</sub> (100 μM) and ClO<sup>-</sup> (100 μM).

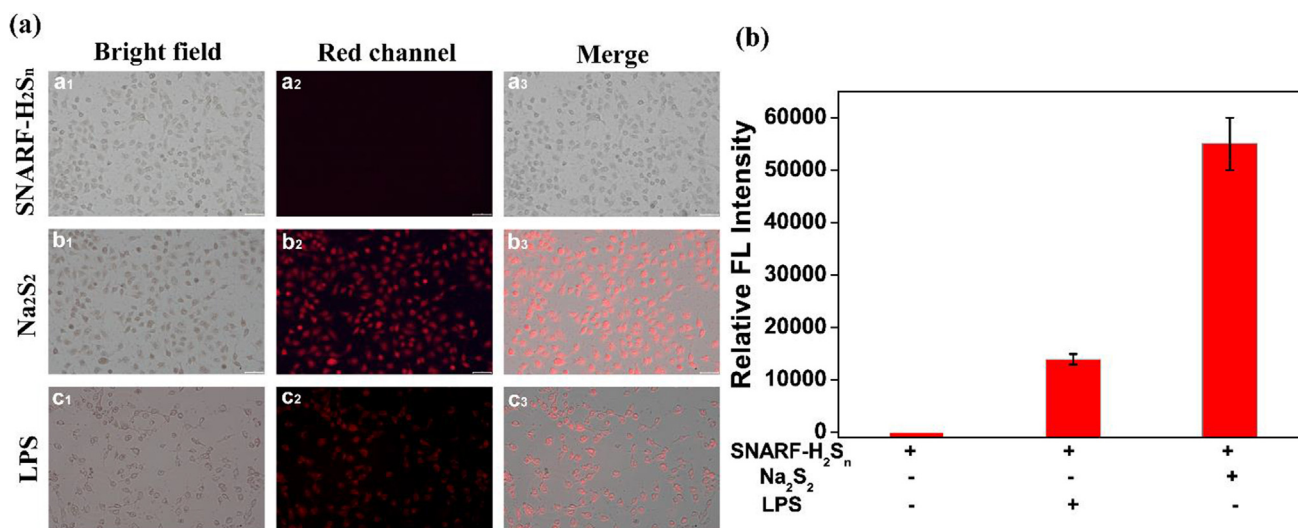


**Fig. 2.** (a) Fluorescence imaging of exogenous/endogenous H<sub>2</sub>S<sub>n</sub> in living A549 cells. (a<sub>1</sub>–a<sub>3</sub>) The cells were incubated with 10 μM SNARF-H<sub>2</sub>S<sub>n</sub> for 30 min; (b<sub>1</sub>–b<sub>3</sub>) the cells stained with 50 μM Na<sub>2</sub>S<sub>2</sub> for 30 min were treated with 10 μM SNARF-H<sub>2</sub>S<sub>n</sub> for another 30 min; (c<sub>1</sub>–c<sub>3</sub>) the cells stimulated with LPS for 12 h, and then incubated with 10 μM SNARF-H<sub>2</sub>S<sub>n</sub> for 30 min. (a<sub>1</sub>, b<sub>1</sub>, c<sub>1</sub>) bright field images; (a<sub>2</sub>, b<sub>2</sub>, c<sub>2</sub>) red channel images; (a<sub>3</sub>, b<sub>3</sub>, c<sub>3</sub>) merged images. Scale bar = 50 μM. (b) Relative fluorescence intensity of red channel in panel A. Values represent mean standard error (n = 3).

fish increased compared to control group, showing the existence of basal H<sub>2</sub>S<sub>n</sub> in vivo. As expected, treatment with Na<sub>2</sub>S<sub>2</sub> and SNARF-H<sub>2</sub>S<sub>n</sub> in turn resulted in further increase in fluorescence signal. To reflect whether SNARF-H<sub>2</sub>S<sub>n</sub> could efficiently response to endogenous H<sub>2</sub>S<sub>n</sub> in zebrafish, we performed the following experiment. While the zebrafish was pretreated with LPS for 12 h followed by a 30 min incubation with SNARF-H<sub>2</sub>S<sub>n</sub>, we observed a pronounced fluorescence enhancement due to the reaction of SNARF-H<sub>2</sub>S<sub>n</sub> with LPS-induced endogenous H<sub>2</sub>S<sub>n</sub> (Fig. 3b). Collectively, all these

results manifested that SNARF-H<sub>2</sub>S<sub>n</sub> could detect and visualize exogenous/endogenous H<sub>2</sub>S<sub>n</sub> activity in zebrafish.

#### 4. Conclusion

In this work, by introducing phenyl 2-(benzoylthio) benzoate as a H<sub>2</sub>S<sub>n</sub>-active trigger to SNARF scaffold, we reported a new type of red-emitting fluorescent probe named SNARF-H<sub>2</sub>S<sub>n</sub> allowed for

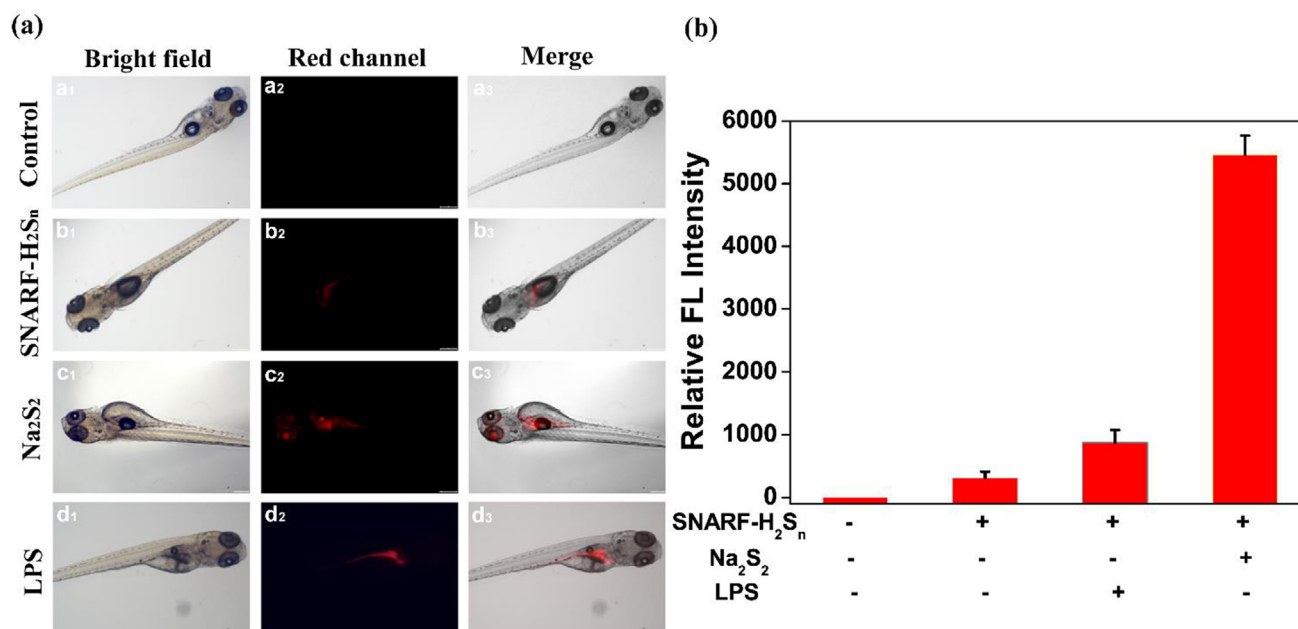


**Fig. 3.** Fluorescence imaging of exogenous/endogenous H<sub>2</sub>S<sub>n</sub> in zebrafish. (a<sub>1</sub>–a<sub>3</sub>) control group; (b<sub>1</sub>–b<sub>3</sub>) the zebrafish were stained with 10 μM SNARF-H<sub>2</sub>S<sub>n</sub> for 30 min; (c<sub>1</sub>–c<sub>3</sub>) the zebrafish were stained with 50 μM Na<sub>2</sub>S<sub>2</sub> for 1 h, and further incubated with 10 μM SNARF-H<sub>2</sub>S<sub>n</sub> for 30 min; (d<sub>1</sub>–d<sub>3</sub>) the zebrafish stimulated with LPS for 12 h, and then incubated with 10 μM SNARF-H<sub>2</sub>S<sub>n</sub> for 30 min. (a<sub>1</sub>, b<sub>1</sub>, c<sub>1</sub>, d<sub>1</sub>) bright field images; (a<sub>2</sub>, b<sub>2</sub>, c<sub>2</sub>, d<sub>2</sub>) red channel images; (a<sub>3</sub>, b<sub>3</sub>, c<sub>3</sub>, d<sub>3</sub>) merged images. Scale bar = 200 μm. (b) Relative fluorescence intensity of red channel in panel A. Values represent mean standard error (n = 3).

detection of H<sub>2</sub>S<sub>n</sub>. On basis of dual reactivity of H<sub>2</sub>S<sub>n</sub>, SNARF-H<sub>2</sub>S<sub>n</sub> was able to respond H<sub>2</sub>S<sub>n</sub> with extreme high selectivity and nanomolar detection limit. Leveraging SNARF-H<sub>2</sub>S<sub>n</sub>, we enabled to track the level fluctuations of exogenous H<sub>2</sub>S<sub>n</sub> in living cells and zebrafish by fluorescence microscope. What's more, our results further revealed that SNARF-H<sub>2</sub>S<sub>n</sub> successfully realized the imaging of endogenous H<sub>2</sub>S<sub>n</sub> stimulated by LPS in vitro and in vivo. We anticipated that SNARF-H<sub>2</sub>S<sub>n</sub> might be a valuable tool for researchers to reveal more information about H<sub>2</sub>S<sub>n</sub>-related diseases.

#### CRedit authorship contribution statement

**Yingying Ma:** Methodology, Data curation, Writing - original draft. **Zhencai Xu:** Methodology, Data curation. **Qi Sun:** Validation, Writing - review & editing, Funding acquisition. **Linlin Wang:** Validation, Writing - review & editing. **Heng Liu:** Conceptualization, Supervision, Project administration, Funding acquisition. **Fabiao Yu:** Supervision, Project administration, Funding acquisition.

#### Declaration of Competing Interest

The authors declare that they have no known competing financial interests or personal relationships that could have appeared to influence the work reported in this paper.

#### Acknowledgement

We thank the Hainan High-Level Talents Project (Grant 2019RC210), National Natural Science Foundation of China (Nos. 21961010, 21775162, 21804102), CAMS Innovation Fund for Medical Sciences (2019-I2M-5-023), Talent Program of Hainan Medical University (Grants XRC190034, XRC180006), Outstanding Young and Middle-aged Scientific Innovation Team of Colleges and Universities of Hubei Province: "Biomass chemical technologies and materials" (Grant No. T201908), Hainan High-Level Talents Program (No. HNRQC201903724) and Hundred-Talent Program (Hainan 2018).

#### Appendix A. Supplementary material

Supplementary data to this article can be found online at <https://doi.org/10.1016/j.saa.2020.119105>.

#### References

- [1] G.I. Giles, K.M. Tasker, C. Jacob, Hypothesis: the role of reactive sulfur species in oxidative stress, *Free. Radical. Bio. Med.* 31 (2001) 1279–1283.
- [2] M.C.H. Gruhke, A.J. Slusarenko, The biology of reactive sulfur species (RSS), *Plant. Physiol. Bioch.* 59 (2012) 98–107.
- [3] C.E. Paulsen, K.S. Carroll, Cysteine-mediated redox signaling: chemistry, biology, and tools for discovery, *Chem. Rev.* 113 (2013) 4633–4679.
- [4] C.T. Yang, L. Chen, S. Xu, J.J. Day, X. Li, M. Xian, Recent development of hydrogen sulfide releasing/stimulating reagents and their potential applications in cancer and glycometabolic disorders, *Front. Pharmacol.* 8 (2017) 664.
- [5] A.L. King, D.J. Lefer, Cytoprotective actions of hydrogen sulfide in ischaemia-reperfusion injury, *Exp. Physiol.* 96 (2011) 840–846.
- [6] H.X. Zhang, S.J. Liu, X.L. Tang, G.L. Duan, X. Ni, X.Y. Zhu, Y.J. Liu, C.N. Wang, H<sub>2</sub>S attenuates LPS-induced acute lung injury by reducing oxidative/nitrosative stress and inflammation, *Cell. Physiol. Biochem.* 40 (2016) 1603–1612.
- [7] S. Sowmya, Y. Swathi, A.L. Yeo, M.L. Shoon, P.K. Moore, M. Bhatia, Hydrogen sulfide: regulatory role on blood pressure in hyperhomocysteinemia, *Vasc. Pharmacol.* 53 (2010) 138–143.
- [8] P. Kamoun, M.C. Belardinelli, A. Chabli, K. Lallouchi, B. Chadefaux-Vekemans, Endogenous hydrogen sulfide overproduction in Down syndrome, *Am. J. Med. Genet. A* 116A (2003) 310–311.
- [9] B.D. Paul, S.H. Snyder, Gasotransmitter hydrogen sulfide signaling in neuronal health and disease, *Biochem. Pharmacol.* 149 (2018) 101–109.
- [10] H.J. Wei, X. Li, X.Q. Tang, Therapeutic benefits of H<sub>2</sub>S in Alzheimer's disease, *J. Clin. Neurosci.* 21 (2014) 1665–1669.
- [11] T.V. Mishanina, M. Libiad, R. Banerjee, Biogenesis of reactive sulfur species for signaling by hydrogen sulfide oxidation pathways, *Nat. Chem. Biol.* 11 (2015) 457–464.
- [12] K. Ono, T. Akaike, T. Sawa, Y. Kumagai, D.A. Wink, D.J. Tantillo, A.J. Hobbs, P. Nagy, M. Xian, J. Lin, J.M. Fukuto, Redox chemistry and chemical biology of H<sub>2</sub>S, hydrosulfides, and derived species: implications of their possible biological activity and utility, *Free. Radical. Bio. Med.* 77 (2014) 82–94.
- [13] T. Ida, T. Sawa, H. Ihara, Y. Tsuchiya, Y. Watanabe, Y. Kumagai, M. Suematsu, H. Motohashi, S. Fujii, T. Matsunaga, M. Yamamoto, K. Ono, N.O. Devarie-Baez, M. Xian, J.M. Fukuto, T. Akaike, Reactive cysteine persulfides and S-polythiolation regulate oxidative stress and redox signaling, *Proc. Natl. Acad. Sci.* 111 (2014) 7606–7611.
- [14] C.M. Park, L. Weerasinghe, J.J. Day, J.M. Fukuto, M. Xian, Persulfides: current knowledge and challenges in chemistry and chemical biology, *Mol. Biosyst.* 11 (2015) 1775–1785.

- [15] C. Debieh-Chouvy, C. Wartelle, F.X. Sauvage, First evidence of the oxidation and regeneration of polysulfides at a gas electrode, under anodic conditions. A study by in situ UV-visible spectroelectrochemistry, *J. Phys. Chem. B* 108 (2004) 18291–18296.
- [16] R. Greiner, Z. Pálkás, K. Bäsell, D. Becher, H. Antelmann, P. Nagy, T.P. Dick, Polysulfides link H<sub>2</sub>S to protein thiol oxidation, *Antioxid. Redox. Signal.* 19 (2013) 1749–1765.
- [17] H. Niu, B. Ni, K. Chen, X. Yang, W. Cao, Y. Ye, Y. Zhao, A long-wavelength-emitting fluorescent probe for simultaneous discrimination of H<sub>2</sub>S/Cys/GSH and its bio-imaging applications, *Talanta* 196 (2019) 145–152.
- [18] L. Yang, H. Xiong, Y. Su, H. Tian, X. Liu, X. Song, A red-emitting water-soluble fluorescent probe for biothiol detection with a large Stokes shift, *Chinese Chem. Lett.* 30 (2019) 563–565.
- [19] Y. Zhang, B. Zhang, Z. Li, L. Wang, X. Ren, Y. Ye, Endoplasmic reticulum targeted fluorescent probe for the detection of hydrogen sulfide based on a twist-blockage strategy, *Org. Biomol. Chem.* 17 (2019) 8778–8783.
- [20] Y.F. Kang, L.Y. Niu, Q.Z. Yang, Fluorescent probes for detection of biothiols based on “aromatic nucleophilic substitution-rearrangement” mechanism, *Chinese Chem. Lett.* 30 (2019) 1791–1798.
- [21] G. Hu, H. Jia, L. Zhao, D.H. Cho, J. Fang, Small molecule fluorescent probes of protein vicinal dithiols, *Chinese Chem. Lett.* 30 (2019) 1704–1716.
- [22] Q. Gong, W. Shi, L. Li, X. Wu, H. Ma, Ultrasensitive fluorescent probes reveal an adverse action of dipeptide peptidase IV and fibroblast activation protein during proliferation of cancer cells, *Anal. Chem.* 88 (2016) 8309–8314.
- [23] Q. Gong, W. Shi, L. Li, H. Ma, Leucine aminopeptidase may contribute to the intrinsic resistance of cancer cells toward cisplatin as revealed by an ultrasensitive fluorescent probe, *Chem. Sci.* 7 (2016) 788–792.
- [24] Q. Fang, X. Yue, S. Han, B. Wang, X. Song, A rapid and sensitive fluorescent probe for detecting hydrogen polysulfides in living cells and zebrafish, *Spectrochim. Acta A. Mol. Biomol. Spectrosc.* 224 (2020) 117410.
- [25] C. Zhang, Q. Sun, L. Zhao, S. Gong, Z. Liu, A BODIPY-based ratiometric probe for sensing and imaging hydrogen polysulfides in living cells, *Spectrochim. Acta A. Mol. Biomol. Spectrosc.* 223 (2019) 117295.
- [26] P. Hou, J. Wang, S. Fu, L. Liu, S. Chen, A new turn-on fluorescent probe with ultra-large fluorescence enhancement for detection of hydrogen polysulfides based on dual quenching strategy, *Spectrochim. Acta A. Mol. Biomol. Spectrosc.* 213 (2019) 342–346.
- [27] K.B. Li, F.Z. Chen, Q.H. Yin, S. Zhang, W. Shi, D.M. Han, A colorimetric and near-infrared fluorescent probe for hydrogen polysulfides and its application in living cells, *Sens. Actuators B-Chem.* 254 (2018) 222–226.
- [28] J. Zhang, X.Y. Zhu, X.X. Hu, H.W. Liu, J. Li, L.L. Feng, X. Yin, X.B. Zhang, W. Tan, Ratiometric two-photon fluorescent probe for in vivo hydrogen polysulfides detection and imaging during lipopolysaccharide-induced acute organs injury, *Anal. Chem.* 88 (2016) 11892–11899.
- [29] F. Yu, M. Gao, M. Li, L. Chen, A dual response near-infrared fluorescent probe for hydrogen polysulfides and superoxide anion detection in cells and in vivo, *Biomaterials* 63 (2015) 93–101.
- [30] M. Gao, F. Yu, H. Chen, L. Chen, Near-infrared fluorescent probe for imaging mitochondrial hydrogen polysulfides in living cells and in vivo, *Anal. Chem.* 87 (2015) 3631–3638.
- [31] C. Liu, W. Chen, W. Shi, B. Peng, Y. Zhao, H. Ma, M. Xian, Rational design and bioimaging applications of highly selective fluorescence probes for hydrogen polysulfides, *J. Am. Chem. Soc.* 136 (2014) 7257–7260.
- [32] W. Chen, E.W. Rosser, D. Zhang, W. Shi, Y. Li, W.J. Dong, H. Ma, D. Hu, M. Xian, A specific nucleophilic ring-opening reaction of aziridines as a unique platform for the construction of hydrogen polysulfides sensors, *Org. Lett.* 17 (2015) 2776–2779.
- [33] J. Chung, H. Li, C.S. Lim, H.M. Kim, J. Yoon, Two-photon imaging of hydrogen polysulfides in living cells and hippocampal tissues, *Sens. Actuators B-Chem.* 322 (2020) 128564.
- [34] H. Zhou, J. Tang, L. Sun, J. Zhang, B. Chen, J. Kan, W. Zhang, J. Zhang, J. Zhou, H<sub>2</sub>S<sub>2</sub>-triggered off-on fluorescent indicator with endoplasmic reticulum targeting for imaging in cells and zebrafishes, *Sens. Actuators B-Chem.* 278 (2019) 64–72.
- [35] Y. Huang, F. Yu, J. Wang, L. Chen, Near-infrared fluorescence probe for in situ detection of superoxide anion and hydrogen polysulfides in mitochondrial oxidative stress, *Anal. Chem.* 88 (2016) 4122–4129.
- [36] X. Gong, X.F. Yang, Y. Zhong, H. Chen, Z. Li, A flavylum-based turn-on fluorescent probe for imaging hydrogen polysulfides in living cells, *RSC Adv.* 6 (2016) 88519–88525.
- [37] H.J. Choi, C.S. Lim, M.K. Cho, J.S. Kang, S.J. Park, S.M. Park, H.M. Kim, A two-photon ratiometric probe for hydrogen polysulfide (H<sub>2</sub>S<sub>n</sub>): Increase in mitochondrial H<sub>2</sub>S<sub>n</sub> production in a Parkinson's disease model, *Sens. Actuators B-Chem.* 283 (2019) 810–819.
- [38] Y. Fang, W. Chen, W. Shi, H. Li, M. Xian, H. Ma, A near-infrared fluorescence off-on probe for sensitive imaging of hydrogen polysulfides in living cells and mice in vivo, *Chem. Commun.* 53 (2017) 8759–8762.
- [39] W. Chen, A. Pacheco, Y. Takano, J.J. Day, K. Hanaoka, M. Xian, A single fluorescent probe to visualize hydrogen sulfide and hydrogen polysulfides with different fluorescence signals, *Angew. Chem. Int. Ed.* 55 (2016) 9993–9996.
- [40] W. Chen, E.W. Rosser, T. Matsunaga, A. Pacheco, T. Akaike, M. Xian, The development of fluorescent probes for visualizing intracellular hydrogen polysulfides, *Angew. Chem. Int. Ed.* 54 (2015) 13961–13965.
- [41] Y. Hou, X.F. Yang, Y. Zhong, Z. Li, Development of fluorescent probes for hydrogen polysulfides by using cinnamate ester as the recognition unit, *Sens. Actuators B-Chem.* 232 (2016) 531–537.
- [42] H. Liu, M.N. Radford, C.T. Yang, W. Chen, M. Xian, Inorganic hydrogen polysulfides: chemistry, chemical biology and detection, *Brit. J. Pharmacol.* 176 (2019) 616–627.
- [43] N. Gupta, S.I. Reja, V. Bhalla, M. Kumar, Fluorescent probes for hydrogen polysulfides (H<sub>2</sub>S<sub>n</sub>, n > 1): from design rationale to applications, *Org. Biomol. Chem.* 15 (2017) 6692–6701.
- [44] X. Zhang, W. Qu, H. Liu, Y. Ma, L. Wang, Q. Sun, F. Yu, Visualizing hydrogen sulfide in living cells and zebrafish using a red-emitting fluorescent probe via selenium-sulfur exchange reaction, *Anal. Chim. Acta.* 1109 (2020) 37–43.